



## A Novel Hybrid Structure of SVC and IPFC for Static Voltage Stability Margin Improvement

Reza Sedaghati and Ahmad Rouhani

Department of Electrical Engineering, Beyza Branch, Islamic Azad University, Beyza, Iran.

### ARTICLE INFO

#### Article history:

Received: 23 July 2013;

Received in revised form:  
24 January 2014;

Accepted: 7 February 2014;

#### Keywords

Loading factor,  
Static voltage stability,  
Continuous power flow,  
Hybrid controller,  
Power injection model.

### ABSTRACT

In this paper, the structure of Hybrid Power Flow Controller (HPFC) is proposed in order to improve static voltage stability characteristics. HPFC forms a hybrid controller using IPFC series converters as a hybrid with existing parallel and passive compensator (SVC) in power system. Utilization of hybrid structures makes it possible to use converters for improving performance of both old and existing compensators in power networks. In this study, the power injection model (PIM) is used to model the hybrid power flow controller in Newton load flow. The aforementioned model is simulated in MATLAB software. The P-V curves of PQ buses of a typical system are evaluated by a continuous power flow (CPF) method to analyse the effect of this controller on static voltage stability characteristics. Meanwhile, SVC as existing devices in the system and UPFC and IPFC as state-of-the-art compensator devices are compared with the proposed hybrid structure. The amount of active and reactive power loss and improvement of loading limit of the system are used as main parameters in our comparison.

© 2014 Elixir All rights reserved

### Introduction

There is an index value called stability margin or loading limit which is used in static voltage stability analysis. System voltage instability can be compensated by increasing voltage stability margin. Thus, voltage collapse studies emphasize on the security of the system and its efficient performance and the main goal of these studies is to reach maximum loading capability of a transmission line [1]. Generally, devices which should be used for solving voltage stability problem are those which make it possible to inject active power and to transmit power with minimum loss. The first devices which were used to solve the voltage instability problem were conventional series and shunt compensators for maximizing transmission capability of a transmission line [2]. Since these devices are not capable of momentarily control and just act in a stepped manner, it was necessary to introduce devices which could control power and voltage momentarily.

In 1998, a new concept of transmission systems called FACTS devices was introduced. A lot of papers about the effect of first generation compensators based on thyristor control (SVC, TCSC, ...) and second generation compensators based on voltage source converter (STATCOM, SSSC, UPFC, IPFC) on voltage stability improvement have been published [3,4]. Second generation of FACTS devices perform compensation independently from network parameters (such as line current, voltage and phase angle) and present better and more smooth characteristics in comparison with first generation. Among them STATCOM and UPFC provide valuable advantages. Both of them are effective in expanding stability margin and providing more performance flexibility [5]. However, UPFC provides more advantages from power loss, voltage profile and increasing loading limit aspects [6]. Nevertheless, installation cost of each of these modern compensation devices in comparison with classic devices is a dissuasive factor for widespread use of these elements [7], and making use of these compensators has become

dependant on the technical and economic specifications of the system. So that for example, investment needed for installing UPFC is a disincentive factor in widespread use of this compensator. Therefore, considering the fact that there exist some old compensators in the network, if some changes can be made to them and a performance similar to the performance of modern devices could be achieved, this will result in many economic advantages for the network.

Hence, in this paper, by joining IPFC series compensation to the existing compensated system by SVC, while reducing investment cost in the system and improving equipment performance of the existing classical compensator [8], it has provided the way to achieve stability properties of static voltage almost similar to the new generation of devices based on voltage source converter (UPFC), yet good economic benefits are established in the network.

### The Hybrid Structure

An applied representation of hybrid power flow controller (HPFC) is shown in Fig. 1. Location of HPFC is in the range of transmission line and in a short distance from high-voltage buses [9]. In this model, a typical hybrid FACTS device, reactive power source with shunt connection called  $B_M$  is used in the middle of HPFC structure. This source can be a switching capacitor bank or a static VAR compensator (SVC), which are both considered as old and existing devices in the system. In this typical structure, two voltage source converters ( $VSC_X$ ,  $VSC_Y$ ) with series connection which are connected to the line by coupling transformers are added to the compensation of the system. These converters are located in two ends of common dc connection terminals. By controlling magnitude and angle of voltages provided by converters, active power flow through line and total reactive power provided for line elements can be controlled simultaneously and independently. Shunt-connected variable susceptance control is synchronized with the converters control, so that major part of reactive power required by the

system is provided. In the proposed hybrid structure, in comparison with the conventional UPFC structure, shunt converter of UPFC is substituted by a switching capacitor or a static VAR compensator (SVC) which existed previously in the system. While its series converters in the HPFC structure is decomposed into two series converters. The capacity used for these two converters in comparison with the capacity of series converter of UPFC seems justifiable from economic point of view due to the omitting of installing capacity of shunt converter.

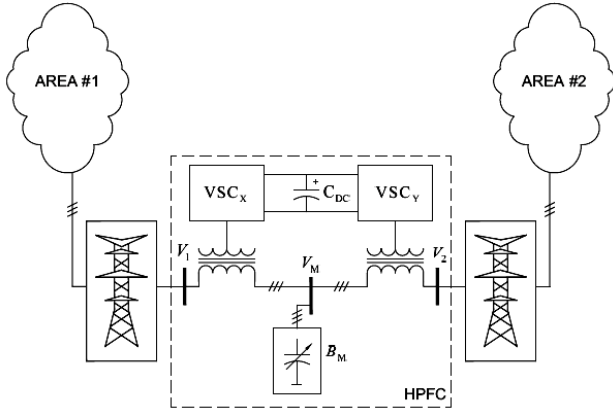


Figure 1. An applied instance of hybrid power flow controller.

Steady state equivalent circuit for HPFC

Equivalent circuit and π injection model of transmission line coupled with series converters

Two series converters coupled with each other in the HPFC structure have a performance similar to the interline power flow controller (IPFC) [10]. As we also recognize IPFC as hybrid compensator, series compensation capacity of HPFC, too, is composed of two SSSCs which are connected to each other by a common dc capacitor (Fig. 2). Usually in steady state analysis of power networks, voltage source converter (SVC) is modeled as a synchronous voltage source which injects a sinusoidal voltage with a controllable phase and magnitude (Fig. 3). In the equivalent circuit shown,  $V_{se_{ij}}$ ,  $V_{se_{ik}}$  are controllable complex voltages of synchronous voltage sources which are defined as  $V_{se_{in}} \angle \delta_{se_{in}}$  ( $n=j,k$ ).  $y_{se_{ij}}$  and  $y_{se_{ik}}$  are the admittances of the transformers which are in series with (i-j), (i-k) lines respectively.

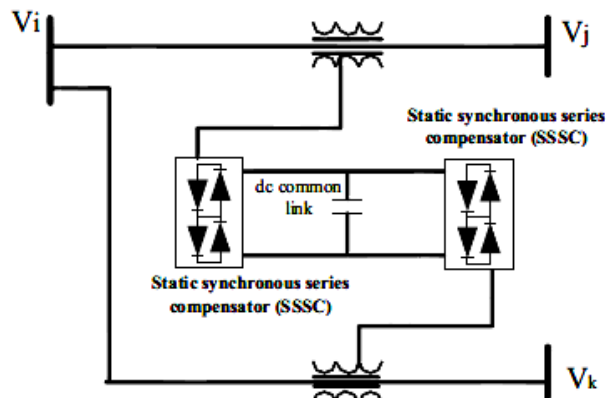


Figure 2. A simple schematic of series compensation part of HPFC

In this paper, in order to omit the need for adding new buses and renumbering them in power flow calculations and in order to keep bus admittance matrix symmetric, power injection model (PIM) of transmission lines coupled with series converter is analyzed for a typical (i-j) line.

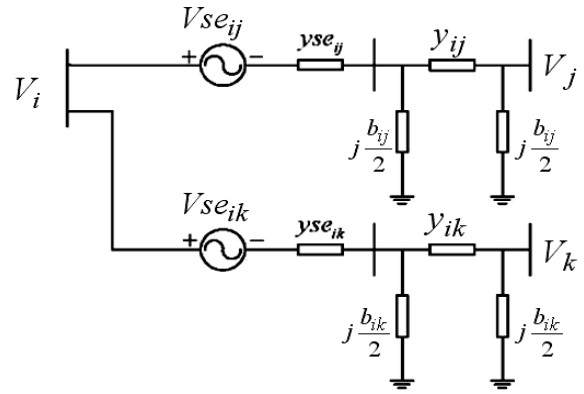


Figure 3. Equivalent circuit of lines coupled with a series converter, based on VSM model.

Y-Δ transform is used to consider the transformer admittance of series converter with admittances of π model of the transmission line. Fig. 4(a) shows a general model of a line coupled with a series converter. Fig. 4(b) shows the Y-Δ transform for the specified region in Fig.4 (a) by a dashed line. Finally, we can obtain the π model of the transmission line coupled with transformer admittance of a series converter in Fig. 4(c) [11]. Equations governing these transformations are of the following form:

$$y'_{ij} = y_{se_{ij}} \cdot y_{ij} / [y_{se_{ij}} + y_{ij} + j \frac{b_{ij}}{2}] \tag{1}$$

$$y_i^{shunt} = j \frac{b_{ij}}{2} \cdot y_{se_{ij}} / [y_{se_{ij}} + y_{ij} + j \frac{b_{ij}}{2}] \tag{2}$$

$$y_{j0} = y_{ij} \cdot \left( j \frac{b_{ij}}{2} \right) / \left[ y_{se_{ij}} + y_{ij} + j \frac{b_{ij}}{2} \right] \tag{3}$$

$$y_j^{shunt} = \left( j \frac{b_{ij}}{2} \right) + y_{ij} \cdot \left( j \frac{b_{ij}}{2} \right) / [y_{se_{ij}} + y_{ij} + j \frac{b_{ij}}{2}] \tag{4}$$

The injected current from the buses i and j of the line coupled with series converters can be obtained from the following equations:

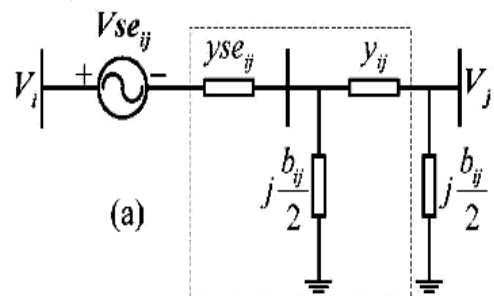
$$I_i = Y_{ii}(V_i - V_{se_{ij}}) + Y_{ij}V_j \tag{5}$$

$$I_j = Y_{ji}(V_i - V_{se_{ij}}) + Y_{jj}V_j$$

Matrix form of the equations above is:

$$\begin{bmatrix} I_i \\ I_j \end{bmatrix} = \begin{bmatrix} Y_{ii} & Y_{ij} \\ Y_{ji} & Y_{jj} \end{bmatrix} \begin{bmatrix} V_i \\ V_j \end{bmatrix} - \begin{bmatrix} Y_{ii}V_{se_{ij}} \\ Y_{ji}V_{se_{ij}} \end{bmatrix} \tag{6}$$

$$\begin{cases} Y_{ii} = y_i^{shunt} + y'_{ij} \\ Y_{ij} = Y_{ji} = -y'_{ij} \\ Y_{jj} = y_j^{shunt} + y'_{ij} \end{cases}$$



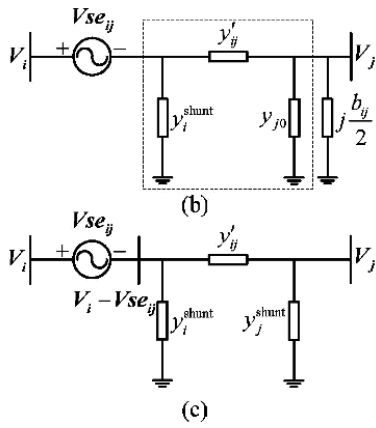


Figure 4. Y-Δ transform process of transmission line coupled with a series converter.

The second part of the right side of the matrix equation (6) can be represented by independent current sources in location of buses i and j (Fig. 5). In this figure, active and reactive power injections in buses i and j are matched with two current sources shown. Therefore, the π injection model of series converter coupled with (i-j) line is shown in Fig. 6.

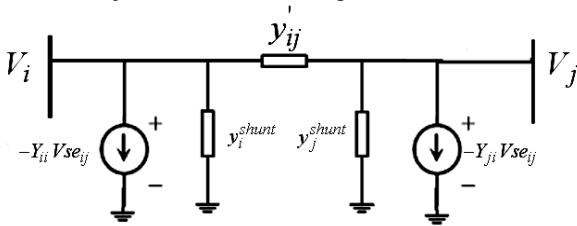


Figure 5. Representation of series branch of IPFC using current sources.

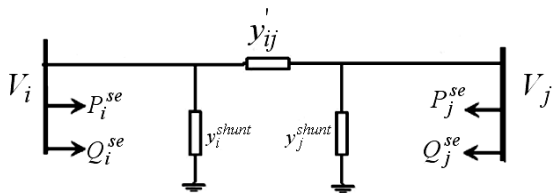


Figure 6. π power injection model of transmission line coupled with a series converter.

Power injection in buses which end at lines coupled with a series converter follows the following equations (Fig. 7):

$$P_i^{se} = \text{Re} \left\{ V_i \left[ -(y'_{ij} + y_{i1}^{shunt}) V_{se_{ij}} - (y'_{ik} + y_{i2}^{shunt}) V_{se_{ik}} \right]^* \right\}$$

$$Q_i^{se} = \text{Im} \left\{ V_i \left[ -(y'_{ij} + y_{i1}^{shunt}) V_{se_{ij}} - (y'_{ik} + y_{i2}^{shunt}) V_{se_{ik}} \right]^* \right\}$$

$$P_n^{se} = \text{Re} \left\{ V_n \left[ (y'_{in}) V_{se_n} \right]^* \right\} \quad (n = j, k)$$

$$Q_n^{se} = \text{Im} \left\{ V_n \left[ (y'_{in}) V_{se_n} \right]^* \right\}$$

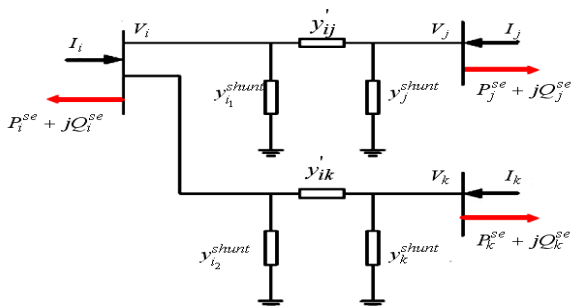


Figure 7. Power injections of coupled series converters in HPFC structure.

The active power exchanged between series converters through common dc connection must be zero under ideal conditions (lossless), therefore we have:

$$P_{dc} = \sum_n P_{ex_n} = 0 \tag{8}$$

$$P_{dc} = - \sum_{n=j,k} \left\{ |V_{se_n}| |V_i| [G_n \cos(\delta_{se_n} - \delta_i) + B_n \sin(\delta_{se_n} - \delta_i)] - |V_{se_n}|^2 G_n + |V_{se_n}| |V_n| [G'_{in} \cos(\delta_{se_n} - \delta_n) + B'_{in} \sin(\delta_{se_n} - \delta_n)] \right\} = 0$$

Where:

$$G'_{in} + jB'_{in} = y'_{in} \tag{9}$$

$$\text{if } n = j, k \rightarrow \begin{cases} G_j + jB_j = y_{i_1}^{shunt} + y'_{ij} \\ G_k + jB_k = y_{i_2}^{shunt} + y'_{ik} \end{cases}$$

**Equivalent circuit and power injection model of the shunt part of HPFC**

The conventional configuration of SVC is a combination of a fixed capacitor and a reactor controlled by thyristor (FC+TCR). In Fig. 8(a) combination of a fixed capacitor and TCR is presented as an equivalent circuit for SVC. In power flow analysis, the total susceptance of SVC may be considered as a variable, thus an extra voltage equation or a reactive power control equation should be added to the set of equations describing the system. In contrast with SVC models which so far have been used in power flow analysis, based on the idea presented in [12], SVC is used in power flow model in a similar way to STATCOM realization. Therefore, presented equivalent circuit for SVC in Fig.8 (a) should be converted to an equivalent circuit of STATCOM, from the power flow analysis point of view. Equivalent representation of SVC is shown in Fig. 8 (b). In this representation, Z<sub>sh</sub> can be obtained from the following equations:

$$Z_{sh} = j[X_{TCR}^{\min} + X_{TCR}^{\max}] / 2 \tag{10}$$

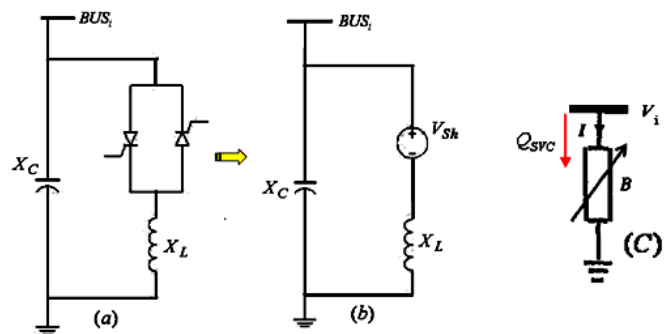


Figure 8. (a,b): equivalent representation of SVC by STATCOM model - (c): Power injection model of SVC.

X<sub>TCR</sub><sup>min</sup>, X<sub>TCR</sub><sup>max</sup> are the lower and upper limits of variable reactance of the TCR branch of SVC's conventional model Fig. 8 (a). Now, variable reactance of TCR branch in Fig. 7(a) can be represented by Z<sub>sh</sub> impedance in series with a variable voltage source (V<sub>sh</sub>). V<sub>sh</sub> source can only inject power to the bus which is connected to it. Therefore, STATCOM model can be applied directly to the SVC. Of course, it should be kept in the mind that instead of the inequality related to V<sub>sh</sub>, X<sub>TCR</sub> inequality must be used in power flow calculations.

**Test System And Analysis Tool**

A 6-bus test system is used in this paper Fig. 9. Having 8 branches, 6 buses along with 6 loads with total of 415 MW and 183 MVAR are the specifications of the system. Results

presented in this paper are obtained from M-file environment of MATLAB software.

$$X_{TCR}^{\min} \leq X_{TCR} \leq X_{TCR}^{\max} \quad (11)$$

$$X_{TCR} = \left| \frac{\bar{V}_{sh} \cdot \bar{Z}_{sh}}{(\bar{V}_i - \bar{V}_{sh})} \right|$$

$$Q_{SVC} = Q_{sh} + Q_c$$

$$\begin{cases} Q_{sh} = B_{sh} [e_i e_{sh} + f_i f_{sh} - e_i^2 - f_i^2] \\ Q_c = -[e_i^2 + f_i^2] \cdot B_c, \quad B_c = \frac{1}{X_c} \end{cases}$$

Devices presented in this paper are modeled in this environment and conventional power flow (PF) calculations and continuous power flow (CPF) with special algorithm (forecasting-correcting) are run on them. All of the loads are considered as fixed power and all of them increase simultaneously under a loading parameter ( $\lambda$ ). Base MVA used in this paper is 100 MVA.

$$P_D = P_{D_o} * (1 + \lambda) \quad (12)$$

$$Q_D = Q_{D_o} * (1 + \lambda)$$

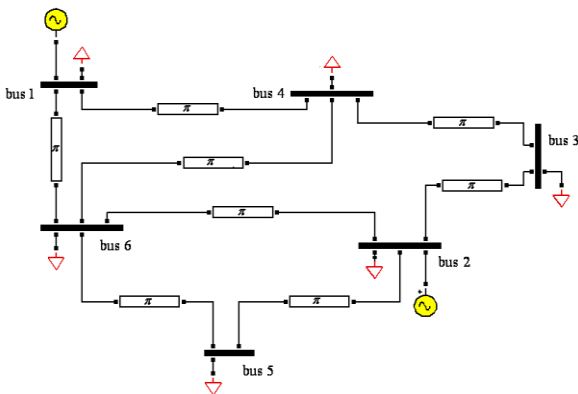


Figure 9. 6-bus Test system.

Simulation Results

Conventional Load Flow

Table 1 shows the Newton load flow results under base loading conditions. The presence of HPFC {SVC+IPFC} in the system is analyzed. SVC in the HPFC structure are considered as old and existing devices in power networks which we have coupled series compensation structure with them in order to improve the performance of existing equipments.

Table 1. Magnitude of bus voltages resulted from Newton-Raphson load flow

Bus	Voltage Magnitude [p.u]					
	Based Case	SVC	STATCOM	SSSC	UPFC	HPFC
1	1.05	1.05	1.05	1.05	1.05	1.05
2	1.04	1.04	1.04	1.04	1.04	1.04
3	0.9919	0.9942	0.9945	0.9913	1.0002	1.0006
4	0.9699	0.9759	0.977	0.9686	0.9928	0.9925
5	0.9208	1	1	0.9372	1	1
6	0.9894	1.0043	1.005	0.9859	1.0398	1.046

Table 2. Installation location of FACTS devices

Compensator	Install Location	
	Bus	Line
SVC	5	---
UPFC	---	(5-6)
IPFC	---	(6-2)-(5-6)
HPFC	5	(6-2)-(5-6)

Continuous Power Flow

Continuous power flow provides a way for complete plotting of static analysis curves (P-V) by continuously changing the value of system loading coefficient ( $\lambda$ ) up to the collapse point.

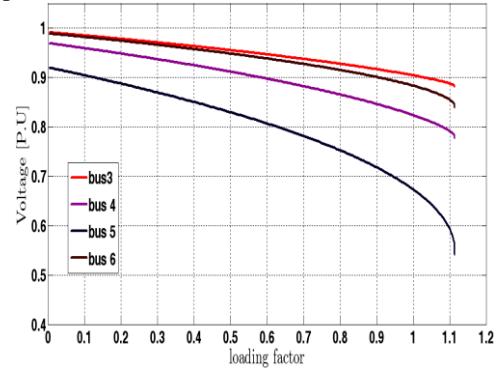


Figure 10. P-V curves of the PQ buses of the system when there is no compensator.

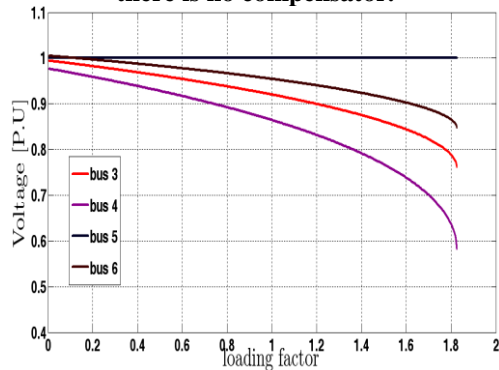


Figure 11. P-V curves of the PQ buses of the system in presence of SVC.

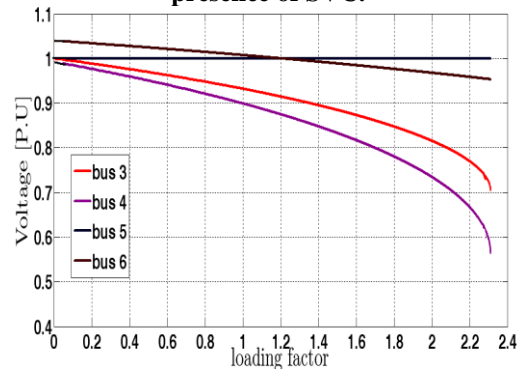


Figure 12. P-V curves of the PQ buses of the system in presence of UPFC.

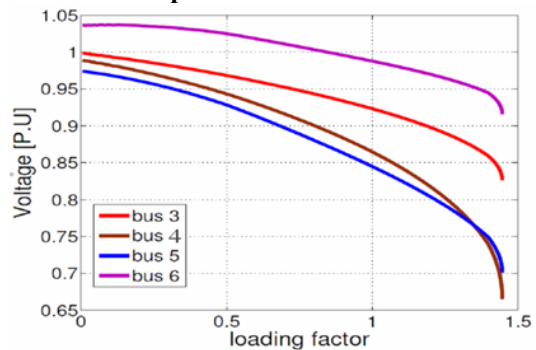


Figure 13. P-V curves of the PQ buses of the system in presence of IPFC.

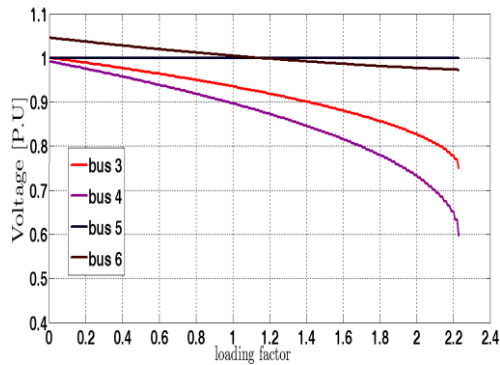


Figure 14. P-V curves of the PQ buses of the system in presence of HPFC.

Table 3. Loading limit and its percent of increment in comparison with base state with presence of FACTS devices

Case	Loading margin	percent of increment
Based State	1.1139	---
SVC	1.7993	61.53
UPFC	2.3108	107.45
IPFC	1.4457	29.78
HPFC	2.241	101.18

**Power Losses**

From the plotted loss curves it is observed that both active and reactive power follow a same pattern when system load is increased. It is clear that UPFC imposes lesser losses for the system in comparison with other devices. Of course considering the amount of total loss, the HPFC structure is in a rank in the middle of shunt FACTS and UPFC devices.

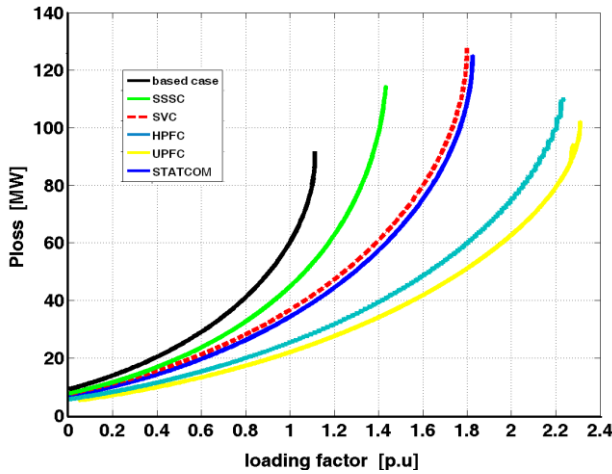


Figure 15. Total active power loss curves with FACTS devices

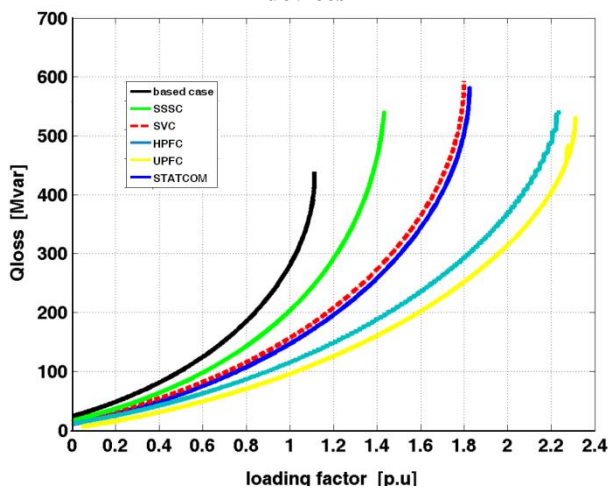


Figure 16. Total reactive power loss curves with FACTS devices.

**Required capacity for series and shunt converters**

In Table 4, two highlighted capacities are related to the existing shunt compensators in the power system which by coupling series compensation to them, the need for utilizing a UPFC with a high capacity of shunt converter has been cancelled. Also, it is observed that by simultaneously using IPFC with existing shunt converters in the system we have become able to increase system loading limit and also to reach lower capacities of series converters in the IPFC structure.

Table 4. Capacity of series and shunt converters in the voltage collapse point

Compensator	MVA Series Converter (5-6)	MVA Series Converter (2-6)	MVA Shunt Converter
SVC	*	*	296.716
UPFC	182.017	*	455.17
IPFC	248.92	349.25	*
HPFC	126.49	128.178	277.62

**Conclusions**

In this paper, a new topology of FACTS devices is proposed. This structure forms a hybrid controller by using series converters in combination with existing shunt compensators in the power system. HPFC could provide static voltage stability characteristics almost similar to that of UPFC just by omitting fairly high capacity of shunt converter in UPFC structure and adding a series compensation capacity to the existing shunt compensators in the system.

**Acknowledgment**

The authors acknowledge financial support from Beyza Branch, Islamic Azad University, Beyza, Iran.

**References**

1. Athamneh, A and Lee, W.J., "The Impact of Using UPFC on Jordanian Power System performance", *39th North American Power Symposium*, pp. 608-614, (NAPS 2007).
2. Bergen, R., *Power Systems Analysis*. Prentice-Hall, New Jersey, 1986.
3. Hingorani, N., "Power Electronics in Electric Utilities: Role of Power Electronics in Future Power Systems," *Proceedings of the IEEE*, vol. 76, no. 4, pp. 481-482, Apr. 1988.
4. Hingorani, N. G. and Gyugyi, L., "Understanding FACTS, Concepts and Technology of Flexible AC Transmission System", IEEE Press, 2000.
5. Kazemi, A; Vahidinasab, V and Mosallanejad, A., "Study of STATCOM and UPFC Controllers for Voltage Stability Evaluated by Saddle-Node Bifurcation Analysis", *IEEE, First International Power and Energy Conference*, pp. 191-195, PECon 2006.
6. Sode-Yome, A; Mithulanathan, N and Lee K.Y., "A Comprehensive Comparison\_ of FACTS Devices for Enhancing Static Voltage Stability", *IEEE, Power Engineering Society General Meeting*, \_pp. 1-8, 2007.
7. Zhang, X. P., "Modeling of the interline power flow controller and the generalized unified power flow controller in Newton power flow," *Proc. Inst. Elect. Eng., Gen., Transm., Distrib.*, vol. 150, no. 3, pp. 268-274, May 2003.
8. Hakimzadeh, M and Sedaghati, R., "Introduction of the Hybrid Power Flow Controller (HPFC) Structure and a Comparison with UPFC", *National Electrical Engineering Conference*, Najafabad, Iran, March 2007.
9. Bebic, J. Z; Lehn, P.W. and Iravani, M.R., "The Hybrid Power Flow Controller A New Concept for Flexible AC Transmission", *IEEE*, pp. 1066-1072, 2006.

10. Jianhong Chen, C; Tjing, T.L and Vilathgamuwa, D.M., "Design of An Interline Power Flow Controller", *14th PSCC*, Sevilla, 24-28 June 2002
11. Yangzan, H and Zengyin, W., "Power System Analysis, vol. I. (3<sup>rd</sup> edition)", Wuhan: *Huazhong University of Science and Technology Press*, 2002, pp. 254-256.
12. Zhang, X.P.; Rehtanz, C, Pal, B., "Flexible Ac Transmission systems: Modeling and Control", © *Springer\_Verlag Berlin Heidelberg*, 2006.